Journal of Traffic and Transportation Engineering 14 (2026) 162-176
doi: 10.17265/2328-2142/2026.04.002

A Preliminary Investigation on the Feasibility of Using a Newly Developed Dynamic Flexural Test to Assess the Fatigue Resistance of Asphalt Mixtures with Stranded Plastic Beads

Liew Pei Wen, Ratnasamy Muniandy, Fauzan Mohd. Jakarni and Salihuddin Hassim
Faculty of Engineering, Universiti Putra Malaysia, Serdang 43400, Selangor, Malaysia

Abstract: Fatigue failure of asphalt pavement roads is getting increasingly rampant with the increasing climate impacts resulting in cracks and potholes. This is supported by many researchers on the subject matter. The specified asphalt mixtures intended for road construction are tested using various methods to quantify fatigue resistance. However, the advent of several reinforcing agents in asphalt mixtures calls for new testing approaches to quantify the fatigue resistance coming from these reinforcing agents. This study explores use of recycled waste plastics that are fabricated into stranded plastic beads as a reinforcing medium to enhance the asphalt layer's fatigue strength. In this study SMA (Stone Mastic Asphalt) with a nominal aggregate size of 20 was selected as it provides a higher Voids in Mineral Aggregate for the plastic bead incorporation and interlocking as compared with the traditional dense graded asphalt mixtures. It is envisioned that the dual end beads with a link enhance the lateral resistance as the end beads get interlocked between compacted aggregates, allowing for better load distribution under heavy axle loads. A four-point dynamic bending testing jig was developed and integrated with a Universal Testing Machine-to evaluate the ability of the bead system to resist flexural deformation through the interlocking SPB (Stranded Plastic Bead) system under various loading conditions. The results showed that the SMA (Stone Mastic Asphalt) mixtures reinforced with SPB were able to resist flexural deformation under higher axle loads with longer rest durations with increased resistance from 11 to 22%. SMA20 with SPB effectively mitigated deflection and delayed crack propagation until it's maximum load-bearing capacity. These findings make it a promising solution for sustainable road construction while simultaneously addressing the plastic waste crisis.

Key words: Flexural deformation, mixture interlocking, reclaimed plastic, stranded plastic beads four-point dynamic bending.

1. Introduction

Malaysia economy is rapidly increasing and the demand for heavy transport trucks is getting crucial. This indirectly involves heavy axle loading on the road pavements. Much research has been conducted to improve the asphalt binder so it can withstand the load and hold the aggregate structure longer in the asphalt pavements. However, the asphalt pavement structures still fail in fatigue and potholes.

Besides the pavement deterioration, an environmental crisis called white pollution is also emerging. Plastic waste increases continuously with the population and is established as the third largest waste source worldwide. Malaysia generates large amounts of plastic waste by the consumption of single-use plastics, and this creates huge challenges for the waste management system. Improper plastic waste management has caused various environmental and human health issues [1]. Besides that, the properties of plastic make it become an essential material for various functions in almost every sector and this has caused the over-consumption of plastic globally. The tendency of people to over-consume

Corresponding author: Ratnasamy Muniandy, Ph.D., Professor, research fields: pavement engineering, asphalt technology.

discard and litter has led to severe environmental pollution [2].

Nevertheless, the properties of plastic to endure and resist degradation made plastic a useful material in road construction. Plastic roads with better performance are produced to reduce the plastic waste caused by over-consumption [3]. With the addition of plastic waste into asphalt binder, the overall pavement performance is improved [4] and with the appropriate amount of plastic added, the mechanical property of asphalt mixtures was improved [5].

Abu et al. found that adding waste plastic fibers to HMA (hot mix asphalt) can improve the rutting and cracking resistance of the asphalt pavement, with a 1% fiber content optimal for high-temperature regions. However, fibers became stiff during mixing, and some protruded after compaction, potentially affecting driving comfort [6]. Besides that, modifying asphalt with waste plastic improves engineering properties, and enhances rutting resistance, and fatigue life. 4% of HDPE (High-Density Polyethylene) is able to enhance stiffness, while 6 to 8% of PET (Polyethylene Terephthalate) can boost the long-term performance of asphalt pavement [7]. However, these methods often face challenges such as phase separation, or limited interlocking effects.

UPM (Universiti Putra Malaysia) developed an innovative product from plastic waste called SPB (Strand Plastic Bead) for the purpose of getting the beads interlocked in the aggregate matrix with the strand link restrain. The research was carried out under the provision of the Ministry of Higher Education research grant. The newly developed diamond shaped plastic bead and link system was designed to replace the 4.75 mm down fine aggregate proportion and at the same time provide an interlocking between the aggregate and the plastic beads [8]. The appropriate features and plastic material of SPB are determined to enable SPB to strengthen the fatigue and rutting resistance of asphalt concrete. It not only integrates plastic waste but also enhances aggregate interlocking and load transfer mechanisms.

Fig. 1 below illustrates the SPB-reinforced asphalt concrete under repeated compressive load (wheel load) and the interlocking between aggregate and SPB. Ordinary asphalt mixtures mostly have lower strength properties due to less sufficient load dispersion within the structure [9]. With the incorporation of SPB, the interlocking mechanism of asphalt concrete was enhanced by the aggregate—SPB interlocking as loads dispersed through the contact points of aggregate and SPB. The SPB was interlocked with aggregate under compressive loads in the asphalt concrete. Greater interlocking was formed with higher compressive loading [10].

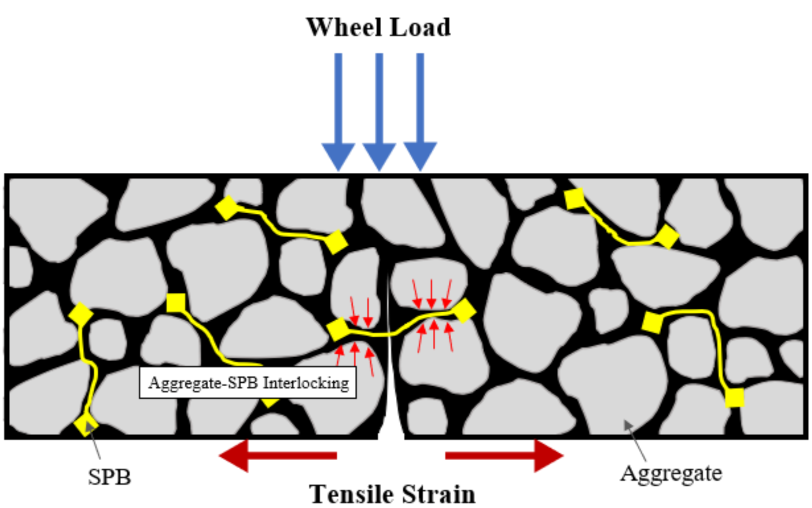

Fig. 1 Schematic view of the interlocking mechanism under wheel load.

Experimental results of various researchers showed that adding 1 to 3% of steel wool fiber improved asphalt mixture performance. However, fiber clustering was observed beyond 3%, increasing air voids and reducing bitumen-aggregate interaction. Higher fiber content which is 7 to 9% led to compression, durability, and stability issues [11]. With 1 to 1.5% waste nylon wire, it improved the SMA's high-temperature stability, crack resistance, and moisture resistance. The reinforcement mechanism works by slowing crack propagation, as the bridging effect reduces energy release and prevents crack development [12]. Wire types of reinforcement are commonly used to reinforce asphalt mixtures by improving tensile strength, crack resistance, and load distribution. However, their effectiveness is often limited by poor dispersion, and stiffness, which can reduce flexibility and lead to localized stress concentrations.

Dynamic Flexural Bending Beam test is commonly conducted on asphalt concrete beams to evaluate the fatigue performance of the specimen. Due to the loading mechanism of the test device, it is unable to measure the flexural strength of the SPB mixture or other reinforced asphalt concrete effectively. The common four-point bending test is frequently performed on FRC (fiber reinforced composites) to evaluate the strength or toughness of the reinforced beam specimen with a simple static loading condition; this type of test evaluates the fracture properties of the sample without the need for cyclic loading conditions [13]. On the other hand, the static loading test is a simplified procedure used to evaluate the fracture properties of asphalt mixtures without the need for cyclic loading conditions [14]. So, it is not commonly performed on asphalt concrete because it's simple that loading configuration does not closely mimic actual traffic conditions, and the static load scale is excessive for asphalt concrete.

A four-point dynamic bending test was developed to enable the beam bending test to be conducted under cyclic loading conditions and more closely simulate real-world traffic conditions. The purpose of this research is to develop a testing method able to measure and quantify the dynamic flexural strength and resistance of the reinforcing plastic bead and link system to the flexural bending under dynamic loading. Thus, a four-point dynamic bending tester for asphalt concrete was developed and incorporated with the UTM (Universal Testing Machine) system to evaluate the flexure strength properties of the plastic bead reinforced mixtures under constant stress mode.

During the constant-strain fatigue test, the stiffness of the sample decreased, and the rate of change of dissipated energy per load cycle increased as the number of load applications increased. Although no crack propagation occurred, microcracks were observed. In contrast, during the constant stress test, crack propagation occurred after a period of crack initiation [15]. As micro cracks healed, the elastic response of the material and the dynamic elastic modulus of the asphalt mixture were restored. Additionally, the flexural stiffness of the asphalt mixture increased after the specimens were subjected to rest periods [16].

2. Materials and Methods

The materials utilized in this study were tested and analyzed in accordance with ASTM (American Society for Testing and Materials) and AASHTO (American Association of State Highway and Transportation Officials) standards wherever possible. The materials such as granite aggregates and the fabricated SPB were carefully selected for the study so as to minimize any unforeseen performance problems. Detailed steps and procedures are explained in the following sections.

2.1 Materials

2.1.1 Asphalt Binder

The 60/70 penetration grade asphalt binder was selected for use in this study as it is traditionally used in Malaysian road construction works. It was observed that the binder properties tested in accordance with

ASTM and AASHTO standards mostly complied with Malaysian local road construction specification (SPJ/KR/2008). All of the tested properties complied with the local authority's (PWD (Public Work Department) Malaysia) requirements as shown in Table 1 below.

2.1.2 Granite Aggregate Source

The crushed granite rock used in this study was outsourced from a quarry in Kajang, Malaysia. To ensure that the aggregates were suitable for use in road construction, the physical and mechanical property tests were conducted to evaluate their quality. The test results, as presented in Table 2, indicate that the granite aggregate possessed excellent engineering properties and complied with the Malaysian road authority's requirements.

SMA (Stone Mastic Asphalt) is formed by a stone skeleton structure with more than 65% coarse aggregate and rich asphalt filler mastic to resist permanent deformation. The skeletal matrix of SMA produced an asphalt mixture with higher VMA (Voids in Mineral Aggregate) compared with the continuously graded aggregate. The plastic beads and links take up some of the VMA present in the SMA mixture to form and enhance the interlocking with aggregate [17]. To provide sufficient room for the plastic bead and links, the mid-range gradation of SMA with a nominal maximum aggregate size of 20 mm was used in this study. The mid-range gradation and specification range of Malaysia PWD for SMA20 [18] is shown in Fig. 2. The percentage passing obtained from the orange line is adopted.

2.1.3 Plastic Beads and Links

Materials used in the fabricating the bead and link system were recycled plastics of thermoset nature that was melted at a temperature above 220 °C and reinforced with fiberglass and remoulded into 3.5 mm diamond shaped beads plastic components using specially designed moulds. The plastic bead and link system were produced into two numbers of 3.5 mm size diamond-shaped beads with a link diameter of 1.0 mm and 20 mm in length. The final fabricated bead and system is as shown in Fig. 3.

Table 1 Testing standards and properties of the selected 60/70 penetration asphalt binder.

Properties	Test method	Value obtained	Requirement
Penetration, 0.1 mm	ASTM D5	61.7	60-70
Softening point, °C	ASTM D36	49.0	48-56
Flash point, °C	ASTM D92	255	≥250
Fire point, °C	ASTM D92	265	n/a
Rotational viscosity @135 °C, Pa.s	ASTM D4402	0.50	≤3.0
Rotational viscosity @165 °C, Pa.s	ASTM D4402	0.13	≤0.8
Rutting factor, test temp. 64 °C @10 rad/s, kPa	AASHTO T315	1.1	≥1.0
Ductility @25 °C, cm	ASTM D113	>100	≥100
Mass loss, %	ASTM D 2872	0.29	≤0.5
Increase in softening point, °C	ASTM D36	1.0	≤10
Retained penetration, %	ASTM D5	68.1	≥52

Table 2 The physical and mechanical properties of crushed granite rock.

Properties	Test method	Value obtained	Requirement
LA abrasion, %	ASTM C131	17.73	≤25
Aggregate impact value, %	ASTM D5874	6.47	≤15
Soundness, %	AASHTO T104	0.50	≤18
Flakiness index, %	ASTM D4791	11.54	≤25
Elongation index, %	ASTM D4791	0.27	≤25
Specific gravity	ASTM C127	2.61	n/a
Specific gravity	ASTM C128	2.64	n/a
Water absorption, %	ASTM C127	0.61	≤2

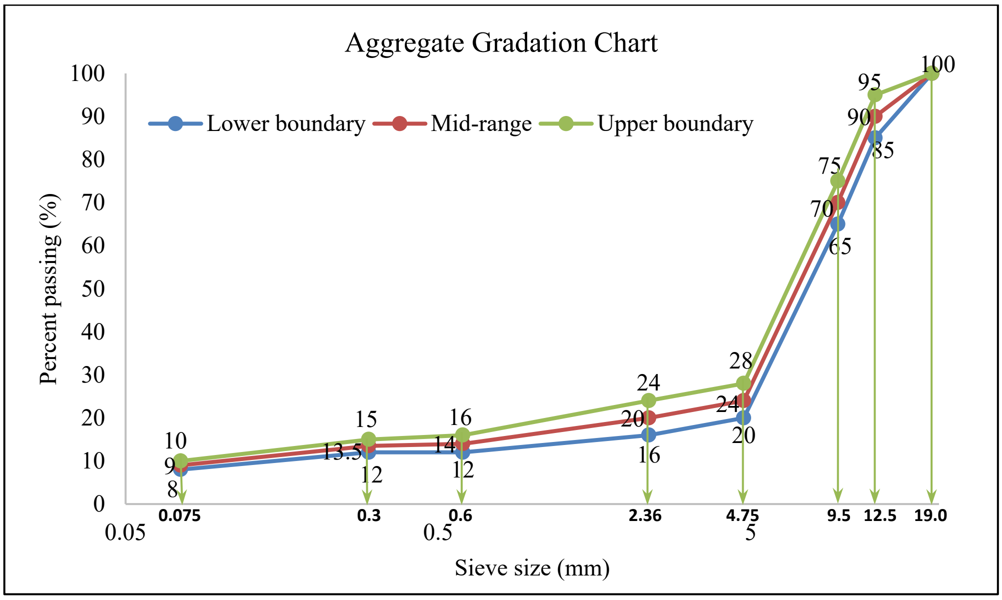

Fig. 2 SMA20 gradation charts.

Fig. 3 Fabricated plastic bead and link.

During the construction of asphalt pavements, high temperatures are typically involved. Therefore, materials that can withstand high temperatures and remain strong throughout the construction process are necessary. Therefore, Nylon 66 Mapex AT0110GN with a melting point above 220 °C was selected as the raw material for the plastic bead and link fabrication. The diamond shape was selected as the design for the beads of SPB to ensure compatibility with the aggregate and promote adhesion with the asphalt binder. Table 3 shows the typical design criteria of plastic bead and link system.

As a reinforcing agent, the linked plastic beads were adopted in the asphalt mixture design to resist the tensile strain under cyclic traffic loading. The linked plastic beads were tested for its tensile strength. The linked plastics was conditioned at 160 °C in the oven for two hours prior to the tensile strength test. The heat-conditioned linked plastic beads were cooled down and tested for their tensile strength in accordance with ASTM D638 along with unconditioned specimens. The purpose of the test was to determine the after effect of heating the plastics and testing after cooling them to room temperature. It is foreseen that the plastic beads and links do not melt at the typical mixing, and laying temperatures of between 155 and 165 °C. However, some softening is expected that gives flexibility in the adaptation and interlocking into the hot aggregate mixtures.

Fig. 4 illustrates the ultimate tensile strengths of the linked plastic beads. As depicted, the unconditioned SPB exhibited a tensile strength value of 68.2 MPa, whereas the SPB conditioned at 160 °C and cooled down to room temperature demonstrated a higher tensile strength of 80.6 MPa. This is expected as reheating and cooling of the thermoset plastics tend to harden further and thus slightly increasing the stiffness of the material. The average tensile strength of the heat-conditioned SPB increased by 18.1% as compared with the unconditioned specimens.

Table 3 Typical design criteria of Strand Plastic Beads (SPB).

Design criteria	Beads	Chain
Length	2.0 mm	Flexible
Diameter	3.5 mm	1.0 mm
Shape	Irregular/diamond shape	-
Surface	Rough	Smooth
Color	White	
Melting point	Above 220 °C	
Material	Thermoplastic	
Material classification	Nylon 66 Mapex AT0110GN	
Specific gravity	1.14	

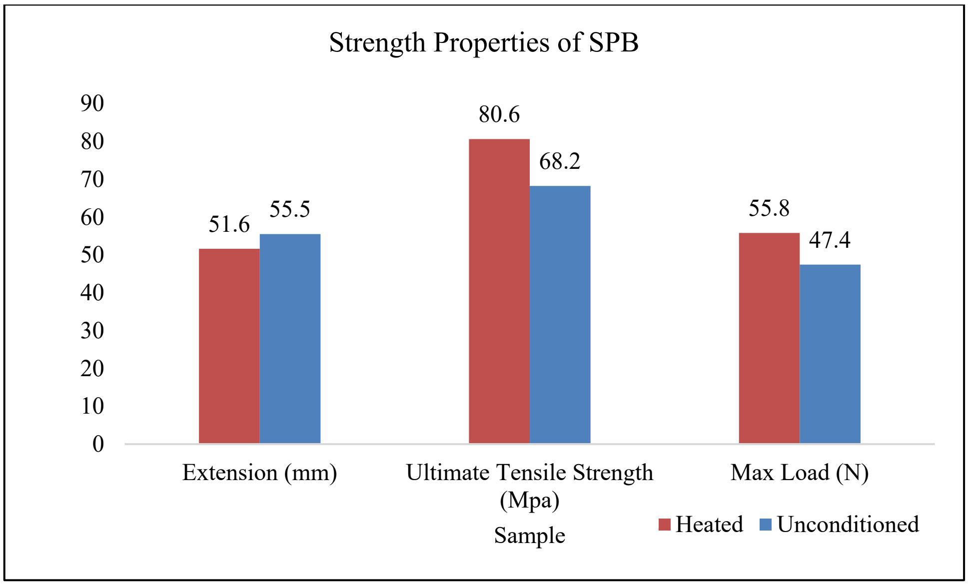

Fig. 4 Strength properties of SPB.

The increase in tensile strength after the heating and cooling process is due to the thermoplastic nature of the material. Heat exposure allows polymer chains to rearrange into a more compact and ordered structure upon cooling, enhancing intermolecular interactions, and increasing strength. The shorter necking and reduced elastic range in conditioned SPB indicate decreased ductility, while the higher ultimate strength before fracture reflects the material's increased structural integrity after thermal conditioning. This is a positive outcome since the asphalt mixture is subjected to mixing temperatures exceeding 160 °C, and the increased tensile strength is expected to provide even greater stiffness strength.

The aggregates passing 4.75 mm and retained on 2.36 mm were selected and proportionally replaced by SPB. The replacement was made by replacing the aggregate with the same volume of SPB. The volume replacement approach was to minimize the influence on the aggregate matrix in the asphalt concrete. Table 4 shows the amounts of aggregate proportionally replaced in SMA20 mid-range gradation, with 10%, 20% and 30% of 4.75-2.36 mm aggregate replaced by SPB through the volume-density method, and the formulated mixtures were named as SMA20 PB-10, PB-20, and PB-30, respectively.

2.2 Methods

2.2.1 Asphalt Mixtures Slab Fabrication

A laboratory slab roller compactor developed by Universiti Putra Malaysia was used in this study for the asphalt mixtures slab fabrication. The slab roller compactor was developed to simulate field compaction for producing compacted slabs with properties closer to field-compacted asphalt concrete. The compactor is capable of compacting slabs with an area of 600 mm by 500 mm and achieving the desired thickness within 15 minutes. The compaction effort can be controlled by adjusting the applied pressure and the number of passes of the roller [19, 20].

The dimension of slabs produced by the slab compactor is 400 mm(W) x 600 mm(L), and the dimension required for a beam specimen is 50 mm(W) x 300 mm(L) with a thickness of 63.4 mm. Therefore, a total number of 12 slabs were fabricated in order to produce 108 beam specimens for the dynamic bending analysis under various testing parameters for the evaluation of the flexure resistance. The quantity of materials necessary for slab fabrication was determined using volume-density calculations based on targeted VTM (Voids in Total Mix) of 4%. The required quantities of materials for slab fabrication are presented in Table 5, including OAC (Optimum Asphalt Content), TMD (Theoretical Maximum Density) and Bulk Density (G_{mb}) of the mixtures.

When comparing the fatigue life under the same loading and temperature conditions, it was found that an increase in beam size resulted in a decrease in fatigue life [21]. To accommodate the newly developed four-point dynamic bending tester, the dimensions of the standard SHRP (Strategic Highway Research Program) beam were modified. The length of the standard SHRP beam was reduced to 300 mm, and the orientation of the beam was adjusted to minimize flexure and allow for the application of greater loads during testing.

Density measurement of the beam specimens is a customary quality control practice for asphalt concrete specimens to ensure that the material properties are consistent. Since the mechanical properties of asphalt mixture are mostly influenced by the volumetric properties of the asphalt mixture [22]. The adopted method involved using a procedure to determine the bulk specific density of a compacted asphalt sample. By maintaining consistent volumetric properties of the beam specimen, the overall results can be obtained with minimal discrepancies.

The notch size can indeed influence the fracture behavior of the asphalt beam. In order to prevent the excessive weakening of the specimen by a deeper notch, a 5 mm shallower notch was introduced at the center of the beam specimen to initiate a controlled crack, as shown in Fig. 5. This pre-cracking method reduced cracking resistance at a specific location, ensuring consistent crack propagation during testing.

The notch depth is approximately 8% of the total beam height (63.5 mm), aligning with standard practices in fatigue testing of bituminous beam specimens according to ASTM D7460. The notch dimensions are

Table 4 Pproportional replacement of SPB in SMA20.

Mix design	% 4.75 mm-2.36 mm aggregate replaced by SPB	Volume to be replaced (cm^3)	Weight of SPB (g)	% SPB by total aggregate weight
Control mix	No replacement	No replacement	n/a	n/a
SMA20 PB-10	10	1.7	2	0.17
SMA20 PB-20	20	3.5	4	0.35
SMA20 PB-30	30	5.2	6	0.52

Table 5 Summary of the quantity of materials required for slabs fabrication.

Mixtures	OAC (%)	TMD	G_{mb}	Weight			
				Aggregate (kg)	Asphalt (kg)	SPB (g)	Total (kg)
Control mix	4.7	2.432	2.339	26.74	1.32	0	28.06
SMA PB-10	4.9	2.387	2.292	26.11	1.35	44.5	27.50
SMA PB-20	5.4	2.395	2.299	26.01	1.49	91.4	27.59
SMA PB-30	5.1	2.373	2.278	25.81	1.39	134.9	27.34

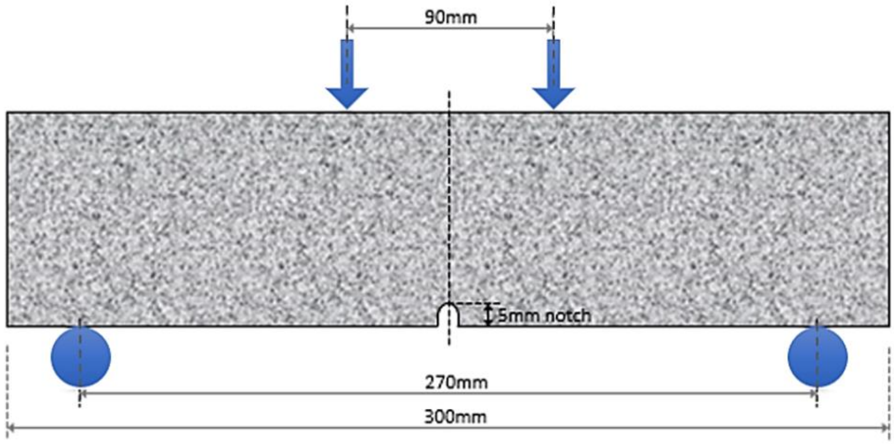

Fig. 5 Beam specimen with 5 mm-notch.

carefully selected to ensure consistent crack initiation while maintaining the structural integrity of the specimen. Additionally, a shallow notch is preferred to concentrate stress within the binder-rich mastic without significantly disrupting the coarse aggregate skeleton of the SMA20.

However, the size and type of notch are critical parameters that affect how materials respond under loading. Further studies are needed to evaluate the impact of varying notch dimensions on fracture behavior more comprehensively to simulate realistic conditions for crack propagation.

2.2.2 Four-Point Dynamic Bending Test

The four-point dynamic bending tester for asphalt concrete beams was developed at UPM to assess the flexure crack resistance of asphalt beam specimens by performing four-point dynamic bending tests. Through the four-point loading, the energy required to deflect and fracture the beam specimen was quantified through the bending behaviour of the specimen [23], which reflects the function of SPB in enhancing the structural interlocking of the asphalt concrete.

The four-point dynamic bending tester was integrated with a UTM (Universal Testing Machine) for beam bending tests. The UTM software was used to set the parameters for the beam bending test and to acquire data. As illustrated in Fig. 6, the four-point bending dynamic tester consists of two parts: the loading span, which is attached to the UTM loading actuator and applies axial load to the beam specimen, and the supporting span, which is designed with roller supports and clamp holders to hold the specimen in the bending test. The roller supports were used to reduce friction between the specimen and the supporting span to ensure that bending occurs only at the two loading points.

The dimensions and features of the four-point dynamic bending tester were carefully considered to ensure its applicability and consistency in performing the dynamic beam bending test. The height of the supporting span should be sufficient to carry the beam specimen and let the LVDT (Linear Variable Differential Transducers) sit underneath the specimen. The LVDTs were situated below the beam specimen held by a pair of magnetic bases to measure the beam deflection during the test. Scrape blocks were positioned beneath the beam specimen during the application of dynamic loading to prevent the specimens from falling and damaging the LVDTs.

In Fig. 7, the loading span consists of loading rollers and a 1.5-inch bolt with a flexible joint, which can be adjusted to fit the UTM actuator. The flexible joint ensures equal distribution of applied loads on both rollers. The loading span has an overall height of 100 mm, including the bolt and rollers, and a length of 150 mm. The distance between the two loading rollers, measured from their centers, is 90 mm.

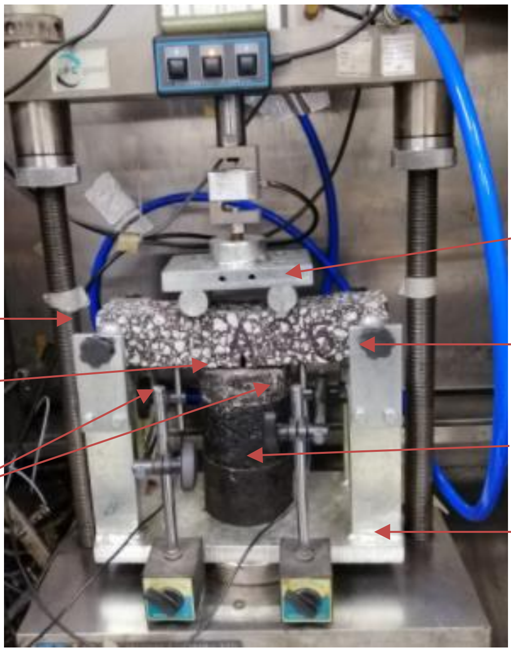

Fig. 6 Specimen and tester setting for four-point dynamic bending test

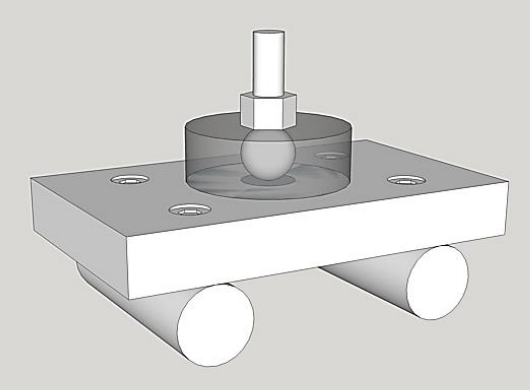

Fig. 7 Loading span of four-point dynamic bending tester.

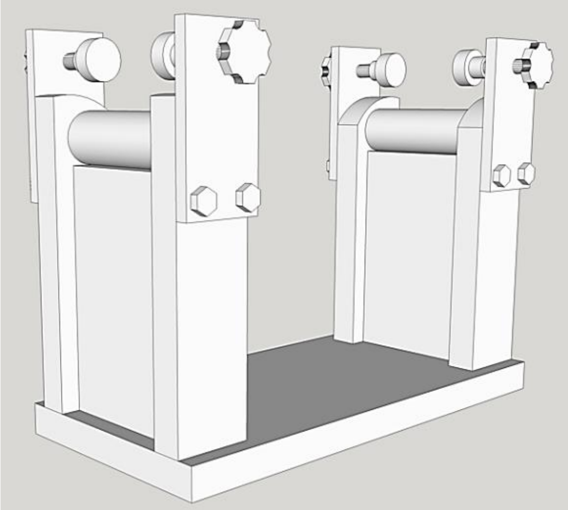

Fig. 8 Supporting span of four-point dynamic bending tester.

Fig. 8 shows that the supporting span comprises supporting rollers and a specimen clamp holder used to secure beam specimens during testing. The supporting span has an overall height of 250 mm, which includes the specimen clamp holder. The distance between the supporting rollers is 270 mm. The supporting span is designed to have a height of 180 mm, measured from the supporting rollers to the base, to allow sufficient space for setting up LVDTs and scraper blocks underneath the beam specimen.

2.2.3 Testing Parameter

At a typical fatigue test temperature of 20 °C, the four-point dynamic bending test was conducted using specified loads and loading frequencies. It is worth noting that the rest periods can have a significant impact on the ability of asphalt concrete to resist fatigue failure [24]. To ensure data integrity, it is necessary to determine the appropriate loads and loading frequencies before conducting the actual four-point dynamic bending test. Additionally, it is important to ensure that the data acquired is reliable, consistent, and capable of obtaining sufficient data before the beam failure occurs.

Preliminary trials of the four-point dynamic bending test were carried out to establish a suitable parameter range. Based on observations of the data obtained, axial loads of 100 kPa, 150 kPa, and 200 kPa were chosen to represent low, medium, and high traffic loadings, respectively. Under constant stress mode, the four-point dynamic bending test was performed using loading frequencies of 1,000 ms (1.0 Hz), 1,500 ms (0.7 Hz), and 2,000 ms (0.5 Hz) to represent high, medium, and low loading frequencies, respectively.

3. Results and Discussion

3.1 Relationship of Strain-Level and SPB Mixtures

Strain level is usually used to indicate the flexural bending or cracking resistance of the asphalt mixture. In this research, the strain values recorded by the UTM data acquisition system during the four-point dynamic bending test were analysed to measure the ability of various SPB mixtures in resisting flexural deformation under various testing parameters. The cracking behavior of the asphalt beam under cyclic loading is illustrated in Figs. 9 to 12. Initially, the beam remains intact before testing (Fig. 9). As the loading cycles increase, slight bending occurs, though microcracks are not yet visible (Fig. 10). With continued cyclic loading, visible cracks begin to form on the beam (Fig. 11). Eventually, crack propagation leads to structural failure as the material loses its integrity (Fig. 12). These images demonstrate the progressive damage and fatigue behavior of the asphalt beam under repeated loading.

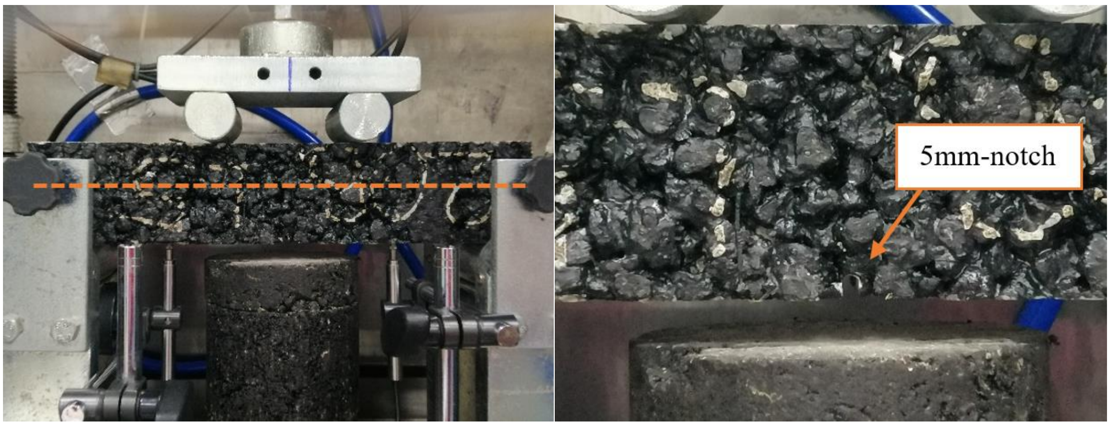

Fig. 9 Beam specimen before testing (initial condition).

Fig. 10 Early stage under cyclic loading—slight bending (microcracks not visible).

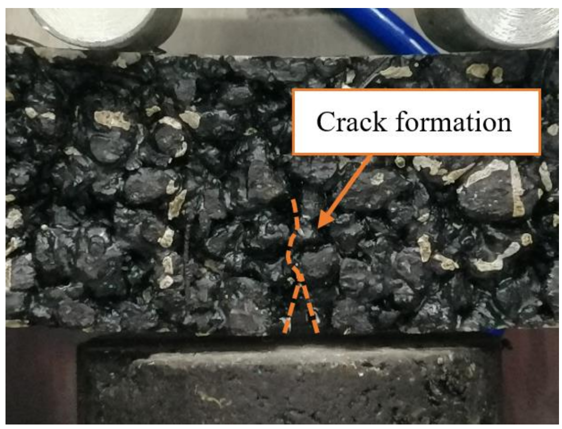

Fig. 11 Crack formation under progressive loading cycles.

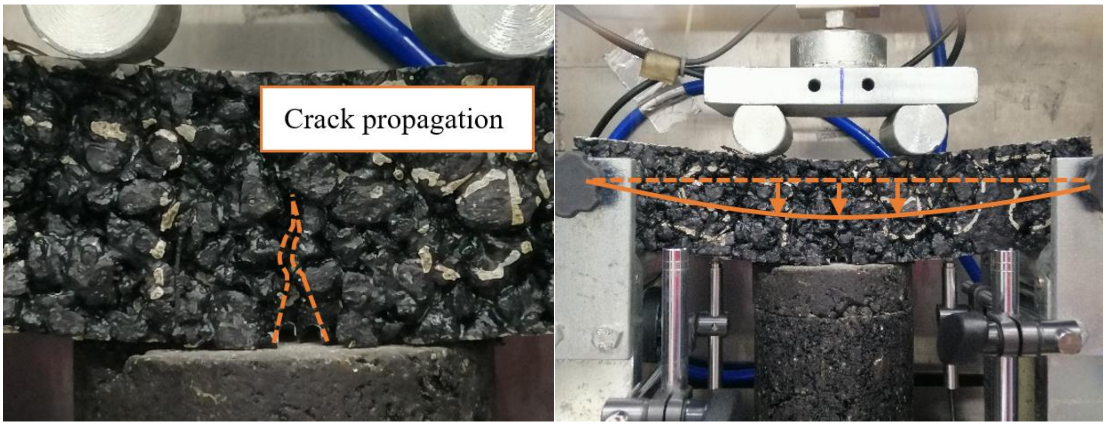

Fig. 12 Crack propagation leading to beam failure.

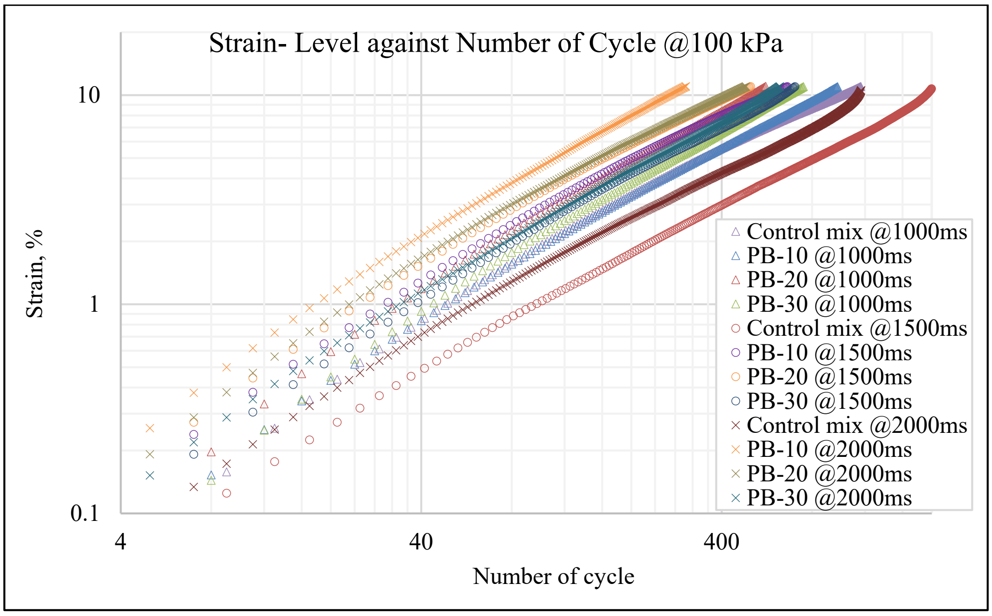

Fig. 13 Plot of strain against number of cycles @100 kPa.

When subjected to a repeated load of 100 kPa, the control mixture exhibited the lowest strain level compared to the SPB mixtures. The curves for the SPB mixtures were steeper than those of the control mix. At low traffic loadings, the SPB mixtures exhibited more deformation than the control mixture. However, the PB10 @1,000 ms was very close to the control samples at 1,000 ms and 1,500 ms. The curves of strain against the number of cycles at low traffic load under loading frequencies of 1,000 ms, 1,500 ms and 2,000 ms are presented in Fig. 13.

Under low traffic loading, the control mixture performed significantly better than the SPB mixtures. However, when subjected to a repeated load of 150 kPa, the curves of the SPB mixtures became smoother and approached the curve of the control mix. On average, the control mix still had the lowest strain level, but the strain level of the SPB mixtures was closer and just slightly higher than the control mix.

The results suggest that under a repeated load of 150 kPa, the SPB formed a stronger interlocking with the aggregate. As the traffic load increased, the contact point between the aggregate and SPB within the stone skeleton structure of SMA experienced greater stress, leading to enhanced interlocking of the aggregate—SPB. It can be seen that the SPB specimens' resistance started closing into the control samples. This is very clear the SPB resistance is kicking in as the impose load gets higher. The curves of strain against the number of cycles at medium traffic load under loading frequencies of 1,000 ms, 1,500 ms and 2,000 ms are presented in Fig. 14.

Further observation was carried out by analysing the resistance curves at an even higher imposed repeated loading of 200 kPa at loading frequencies of 1,500 ms and 2,000 ms. The SPB mixtures outperformed the control mixtures. The curves for the SPB mixtures were smoother than those for the control mix, and the SPB mixtures exhibited lower strain levels. At a loading frequency of 2,000 ms, the SPB mixtures exhibited the lowest strain level.

The results suggest that when the asphalt beam is subjected to higher repeated loading of 200 kPa the imposed stress was dispersed within the granular structure of the beam specimen; the interlocking between the aggregate and SPB started showing resistance. With longer rest periods of 1,500 ms and 2,000 ms, most of the SPB mixtures outperformed the control mix under the repeated load of 200 kPa. The SPB continuously interlocked with the aggregate under the greater repeated loads, thereby resisting deflection and cracking before the SPB reached its maximum loading capacity. It is observed that the resistance of the various percentages of SPB started to increase as the imposed load increased. This phenomenon can be seen from Figs. 13 to 15 with most of the SPB samples performing better the control mixtures at 1,500 ms and 2,000 ms. The strain levels of PB 10 samples at 1,000 ms and 2,000 ms showed a decreasing trend towards the 150 cycles as compared with control mix at 1,000 ms. A strong possibility is seen here that the fatigue resistance of the SPB may increase with much more reduced strain level beyond the 150 cycles as there are already merging. The curves of strain against number of cycles at high traffic loading under loading frequency of 1,000 ms, 1,500 ms and 2,000 ms are presented in Figure 15.

3.3 Average Unit Strain per Cycle Under Various Testing Parameters

The relationship between the flexural strength of SPB mixtures under various loading conditions was evaluated through the average unit strain per cycle. The ability of the SPB mixtures to resist flexural deformation was observed through the average unit strain per cycle under various testing conditions, as presented in Fig. 16.

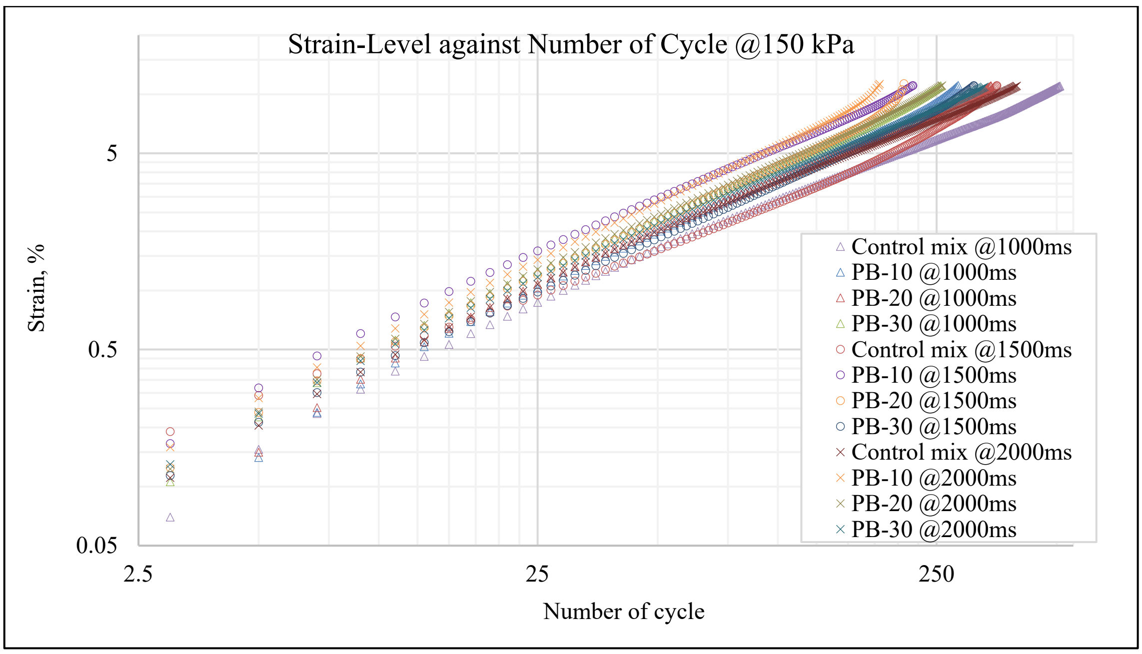

Fig. 14 Plot of strain against number of cycles @150 kPa.

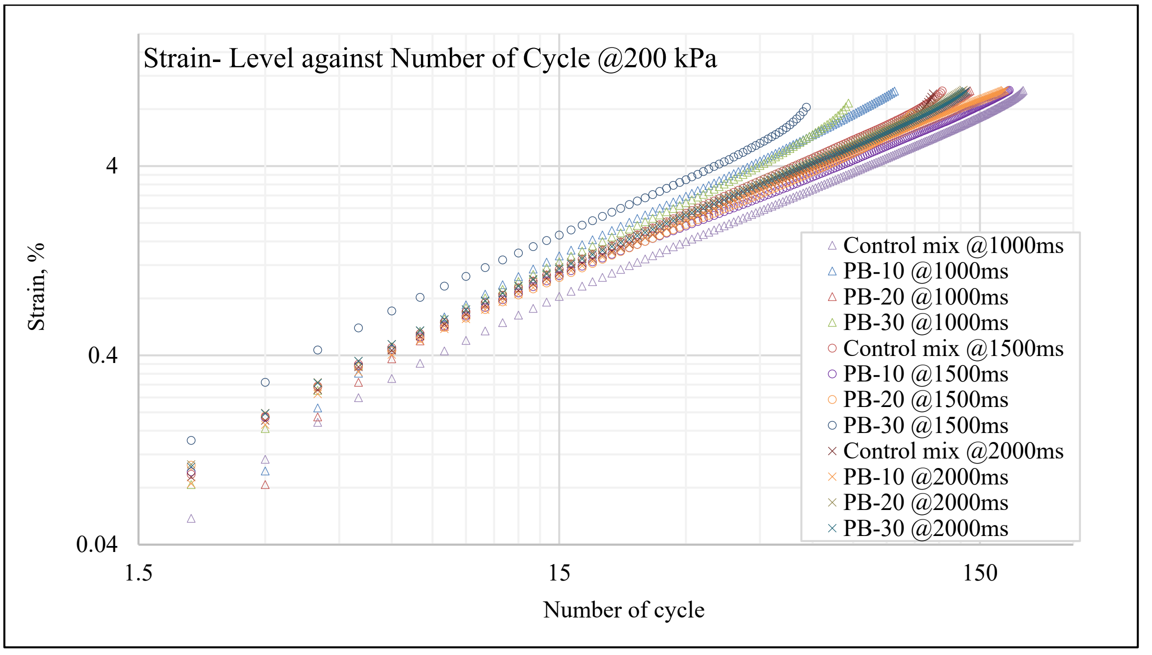

Fig. 15 Plot of strain against number of cycles @200 kPa.

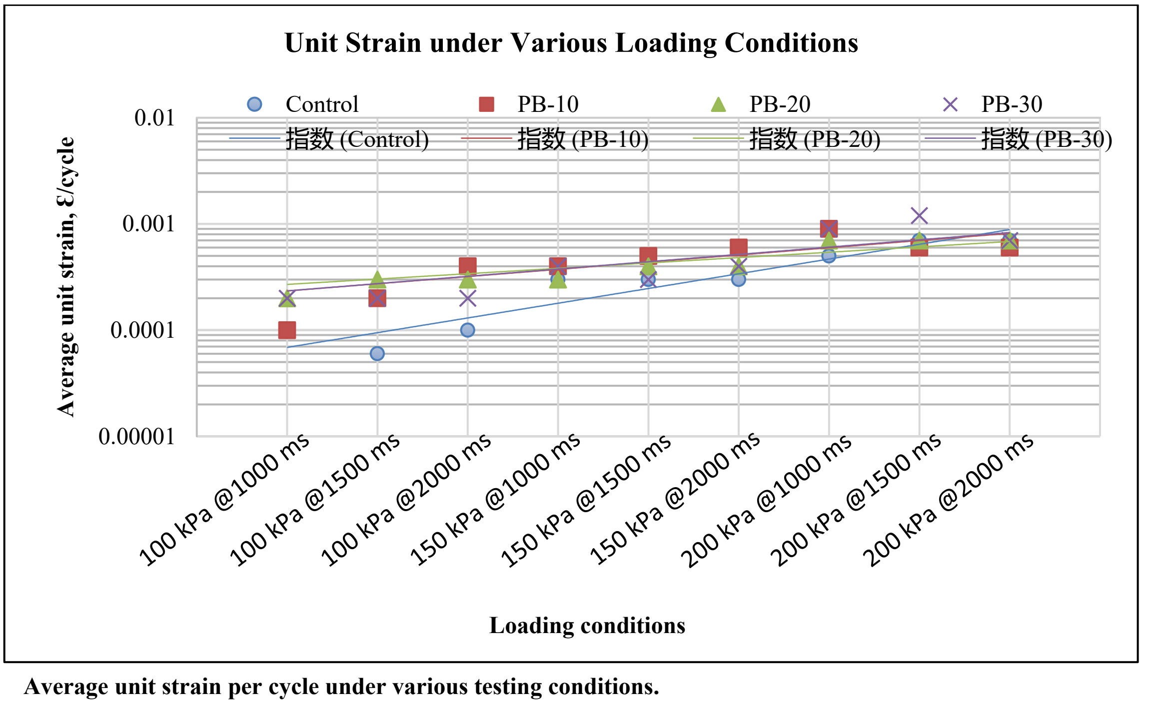

Fig. 16 Average unit strain per cycle under various testing conditions.

The average unit strain per cycle under various testing parameters was evaluated to find out the resistance of SPB mixtures to flexural deformation. It can be observed that the overall unit strain per cycle increases with an increase in the repeated loads and rest duration. However, the exponential lines for SPB mixtures show a moderate flattening effect as the repeated loads and rest duration increase. The flexural deformation for SPB mixtures is lower than the control mix at a high cyclic load of 200 kPa and loading frequency of 2,000 ms. This indicates that the SPB mixtures have a better ability to resist flexural deformation under higher applied loads and longer rest durations.

Table 6 Percentage change of unit strain under various loading conditions.

Mixtures	Unit Strain $_{Initial}$	Unit Strain $_{Final}$	% change
Control	0.00007	0.0009	92.0
PB-10	0.00024	0.0008	70.0
PB-20	0.00027	0.0007	61.4
PB-30	0.00024	0.0008	70.0

At low and medium traffic loading, the asphalt binding strength is still working well in holding the aggregate structure of the asphalt concrete. However, as the traffic loads get higher and higher, the strength of the asphalt binder starts to fail, and the interlocking of SPB and aggregate will take place in reinforcing and stabilizing the granular structure of the asphalt concrete. When the higher traffic load is dispersed within the granular structure of the asphalt mixture, the interlocking strength between aggregate and SPB is enhanced and stronger. The SPB continuously interlock with the aggregate under the high repeated loads to resist the flexural deformation until the SPB reaches their maximum capacity.

Table 6 shows the changes in the unit strain of the beam specimens under various applied loads and loading frequencies. The changes in the unit strain per cycle for the control sample showed 92%, while PB-10 and PB-30 showed a 70% change. The PB-20 showed a 61.2% change only. These show increased fatigue-resistant potential of the SPB with PB-10, 20 and 30 as the axle load increased. These show the SPB asphalt concrete would be an ideal solution for the heavy creeping trucks on the road.

4. Conclusions

Mixtures with SPB exhibited enhanced fatigue resistance due to the interlocking of the SPB within the compacted aggregates, resulting in superior performance under repeated high-magnitude loading. As the applied load increased, especially during longer rest periods, the mixtures demonstrated greater resistance to flexural deformation. This indicates that adding SPB can significantly improve the fatigue performance of SMA mixtures, particularly in high-traffic conditions.

The aggregate—SPB interlocked structure facilitates the effective transfer and dispersion of traffic loads to lower pavement layers. Under increasing loads, stronger interlocking forms at aggregate—SPB contact points, enhancing the mixtures' ability to resist flexural stress. For instance, the unit strain per cycle for the control sample changed by 92%, while PB-10, PB-20, and PB-30 exhibited changes of 70%, 61.2%, and approximately 11-22% increased resilience with rising axle loads.

Moreover, longer rest periods (i.e., lower loading frequencies) further improved resistance to flexural stress across most SPB mixtures. These findings highlight SPB's potential to reinforce asphalt pavements, particularly against heavy axle loads from slow-moving trucks. Using recycled plastic waste in pavements could also address environmental challenges, utilizing about 5.5 tons of plastic waste per 10 km of resurfaced pavement per lane. This approach not only helps mitigate the global plastic crisis but also enhances pavement durability.

The load levels used in the study are still at the lower end and more studies should be carried out to investigate the SPB fatigue resistance at much higher loads beyond 200 kPa.

Acknowledgement

The authors would like to acknowledge the Research Management Center, Universiti Putra Malaysia for the continuous support on this research and an initial grant was provided by the Ministry of Higher Education in the form FRGS (Fundamental Research Grant Scheme) and PRGS (Prototype Research Grant Scheme) prior to this study.

References

[1] Chen, H. L., Nath, T. K., Chong, S., Foo, V., Gibbins, C., and Lechner, A. M. 2021. "The Plastic Waste Problem in Malaysia: Management, Recycling and Disposal of Local and Global Plastic Waste." *SN Applied Sciences* 3: Article 437.

[2] Guern, L. 2019. "When the Mermaids Cry: The Great Plastic Tide." Coastal Care. https://plastic-pollution.org/.

[3] Manju, R., Sathya, S., and Sheema, K. 2017. "Use of Plastic Waste in Bituminous Pavement." *International Journal of ChemTech Research* 10 (8): 804-11.

[4] Limantara, A. D., Gardjito, E., Ridwan, A., Subiyanto, B., Raharjo, D., Santoso, A., Heryanto, B., and Sudarmanto, H. L. 2019. "Comparative Study of Bio-Asphalt, Coconut Shell Distillation TAR, and Plastic Road in Terms of Construction, Economical, and Regulatory Aspects." *Journal of Physics: Conference Series 1364* (1): 012058.

[5] Kader, S. A., Jaya, R. P., Yaacob, H., Hainin, M. R., Hassan, N. A., Ibrahim, M. H., Mohamed, A. A., and Ichwana. 2017. "Stability and Volumetric Properties of Asphalt Mixture Containing Waste Plastic." MATEC Web of Conferences.

[6] Abu, A., A. M., and Jung, S. J. 2019. "Investigation of Reinforcing Flexible Pavements with Waste Plastic Fibers in Ras Al Khaimah, UAE." *Road Materials and Pavement Design* 21 (6): 1753-62. https://doi.org/10.1080/14680629.2019.1566086.

[7] Mashaan, N. S., Rezagholilou, A., and Nikraz, H. 2019. "Waste Plastic as Additive in Asphalt Pavement Reinforcement: A Review." Proceedings of the 18th AAPA International Flexible Pavements Conference, Sydney, New South Wales, Australia.

[8] Ahmad, N., Muniandy, R., Hassim, S., and Aburkaba, E. 2013. "Development of Interlocking Chained Plasti-Beads for Use in Stone Mastic Asphalt." *Australian Journal of Basic and Applied Sciences* 7 (4): 466-74.

[9] Kim, M.-J., Kim, S., Yoo, D.-Y., and Shin, H.-O. 2018. "Enhancing Mechanical Properties of Asphalt Concrete Using Synthetic Fibers." *Elsevier: Construction and Building Materials* 178: 233-43.

[10] Park, P., El-Tawil, S., Park, S.-Y., and Naaman, A. E. 2015. "Cracking Resistance of Fiber Reinforced Asphalt Concrete at -20 °C." *Elsevier: Construction and Building Materials* 81: 47-57.

[11] Köfteci, S. 2018. "Experimental Study Concerning Iron Wire Fiber Reinforced Asphalt Concrete." *Teknik Dergi* 2018: 8515-35. https://doi.org/10.18400/tekderg.350135.

[12] Yin, J., and Wu, W. 2018. "Utilization of Waste Nylon Wire in Stone Matrix Asphalt Mixtures." *Waste Management* 78: 948-54. https://doi.org/10.1016/j.wasman.2018.06.055.

[13] Saha, G., and Biligiri, K. P. 2016. "Homothetic Behaviour Investigation on Fracture Toughness of Asphalt Mixtures Using Semicircular Bending Test." *Construction and Building Materials* 114: 423-33. https://doi.org/10.1016/j.conbuildmat.2016.03.169.

[14] Saha, G., and Biligiri, K. P. 2016. "Fracture Properties of Asphalt Mixtures Using Semi-Circular Bending Test: A State-of-the-Art Review and Future Research." *Construction and Building Materials* 105: 103-12. https://doi.org/10.1016/j.conbuildmat.2015.12.046.

[15] Little, D. N., Lytton, R. L., Williams, D., and Chen, C. W. 2001. *Microdamage Healing in Asphalt Concrete, Volume 1: Microdamage and Microdamage Healing, Project Summary Report*.

[16] Daniel, J. S., and Kim, Y. R. 2014. "Laboratory Evaluation of Fatigue Damage Constitutive Modeling of Asphalt Concrete." *EWSHM—7th European Workshop on Structural Health Monitoring* 13 (6): 434-40.

[17] Ahmad, N. F. 2014. *Performance of Stone Mastic Asphalt Mixture Reinforced with Newly Developed Interlocking Chained Plasti-Beads.* Universiti Putra Malaysia.

[18] Jabatan Kerja Raya Malaysia. 2008. *Standard Specification for Road Works, Section 4: Flexible Pavement, JKR/SPJ/2008-S4.*

[19] Muniandy, R., Jakarni, F. M., Hassim, S., and Selim, A. 2008. "Determination of SMA Slab Properties Using a Newly Developed Roller Compactor (Turamesin)." In *First International Symposium on Transportation and Development Innovative Best Practices*, pp. 505-10.

[20] Muniandy, R., Jakarni, F. M., Hassim, S., and Mahmud, A. R. 2008. "A Newly Developed Laboratory Slab Roller Compactor (Turamesin): An Overview." *International Journal of Engineering, Transactions A: Basics* 21 (2): 133-42.

[21] Li, N., Molenaar, A., Van, D. V., Pronk, A., and Wu, S. 2012. "Investigation into the Size Effect on Four-Point Bending Fatigue Tests." In *3rd Conference on Four-Point Bending*, pp. 35-47.

[22] Molenaar, A., and Li, N. 2014. "Prediction of Compressive and Tensile Strength of Asphalt Concrete." *International Journal of Pavement Research and Technology* 7 (5): 324-30.

[23] Banthia, N., and Trottier, J. 2016. "Test Methods for Flexural Toughness Characterization of FRC." *Aci Materials Journal*.

[24] Pérez-Jiménez, F. E., Miró, R., Botella, R., López-Montero, T., and Martínez, A. H. 2022. "The Effect of Temperature, Rest Periods and Ageing on the Response of Bituminous Materials in Fatigue Tests: Considerations and Proposals on Analytical Dimensioning Models." *Materials (Basel)* 15 (3): 790.